ACS OMEGA

Open Access

http://pubs.acs.org/journal/acsodf

Article

Novel Tapentadol Screen-Printed Carbon Sensor Integrated Copper Oxide Nanostructure

Razan M. Snari, Zehbah A. Al-Ahmed, Arwa Alharbi, Abdullah A. A. Sari, Hanadi A. Katouah, Reem Shah, Fawaz A. Saad, Fathy Shaaban, and Nashwa M. El-Metwaly*

Cite This: *ACS Omega* 2025, 10, 2897−2907

Read Online

ACCESS | Metrics & More | Article Recommendations | Supporting Information

ABSTRACT: The present study described the fabrication and electroanalytical performance of planar screen-printed disposable sensors based on copper oxide nanoparticles (CuONPs/SPEs) for the voltammetric determination of tapentadol (TAP) in its marketed pharmaceutical products and biological fluids. CuONPs exhibited electrochemical activity against the electrooxidation of TAP with an anodic peak at 0.84 V in the BR buffer at pH 5. The electroanalytical investigations and molecular orbital calculations pointed out the oxidation of the tertiary amine group within the TAP moiety with the transfer of two electrons and protons during the oxidation of the TAP molecule at the CuONPs/SPEs surface. Linear calibration graphs were constructed covering the TAP concentration ranging from 0.83 to 738 ng mL^{-1} with a limit of detection (LOD) value up to 0.24 ng mL^{-1}. The disposable printed sensor based on CuONPs offered high measurement and fabrication reproducibility with a prolonged lifetime of 6 months. Improved performance toward TAP was recorded without noticeable interference from degradation products, additives, excipients, uric acid, and ascorbic acid. Moreover, tapentadol and paracetamol (PC) can be simultaneously quantified. The CuONPs/SPEs were applied for monitoring TAP residues and in vitro dissolution studies of TAP in commercial pharmaceutical formulations.

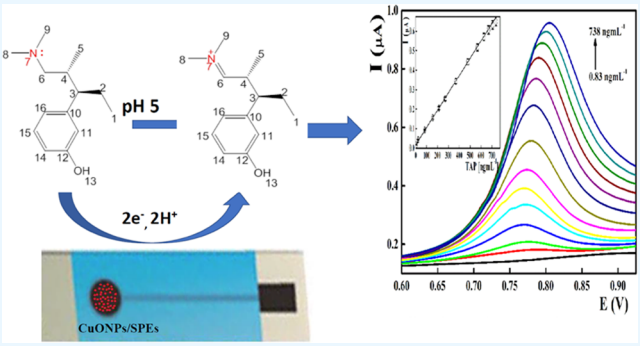

1. INTRODUCTION

Pain, an unpleasant response feeling, can manifest as acute or chronic. Effective pain management relies on a range of pharmacological interventions, including nonopioid and opioid analgesics. Tapentadol (TAP) is an opioid analgesic that acts as an inhibitor of norepinephrine reuptake and a μ-agonist receptor in the central nervous system.[1,2] TAP received FDA approval in 2008, followed by approvals in the United Kingdom and Europe in 2010, and it is now available in over 56 countries worldwide.[3,4] TAP is administered for the efficient treatment of severe, acute, moderate, and chronic pain, such as neuropathic and musculoskeletal pain (lower back, knee, or hip osteoarthritis). Clinical trials and long-term efficacy studies demonstrate sustained pain management without evidence of drug tolerance for up to 2 years of continued treatment.[5] Due to its dual synergistic action, TAP exhibits broad analgesic properties and an exceptionally potent pain-reducing effect, falling somewhere between morphine and tramadol. It achieves this without relying on active metabolites and has minimal drug interactions, as approximately 99% of TAP metabolites are excreted by the kidneys.[6,7] Moreover, TAP is well tolerated and associated with less common side effects and a lower fatality rate compared to other opioid analgesics like morphine, oxycodone, and hydrocodone.[8] The common side effects of TAP are vomiting, dizziness, nausea, headaches, somnolence, and decreased appetite. Additionally, less common effects related to the central nervous system including sedation, depressed mood, respiratory depression, and drug withdrawal syndrome were also reported.[2] However, abusive drug practices still pose risks of opioid overdose and fatality. Detecting tapentadol in urine using existing toxicology screen tests is challenging because many of the available tests are limited to certain μ-agonist drugs and lack specificity and sensitivity to others.[9,10]

Tapentadol is not official in any pharmacopeia; however, few spectrophotometric and chromatographic methods were reported for assaying TAP in bulk and formulated samples.[2] Chromatographic techniques such as RP-HPLC,[11−1213], HPTLC,[14] and HPLC-MS/MS[15−17] were reported for the quantification of tapentadol in complex samples. UV spectrophotometric methods,[18,19] Q-absorbance ratio spec-

Received: October 6, 2024
Revised: January 1, 2025
Accepted: January 6, 2025
Published: January 16, 2025

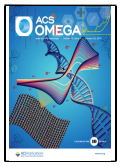

trometry,[20] and ratio-spectra derivative spectrophotometry were reported.[21] In addition, a kinetic spectrophotometric method to assess tapentadol in tablets and spiked urine samples showed a linearity of 2−12 μg mL^{-1}.[22] Moreover, a stability-indicating spectrofluorimetric approach was introduced for a sensitive measuring of TAP in bulk and pharmaceutical formulations.[23] Chromatographic approaches effectively separate and monitor the pharmaceutical compounds, but they are expensive, with complicated pretreatment protocols and the requirement of skilled operators.[24] Spectrometric measurements are usually applied for authentic pharmaceutical formulations containing higher analyte concentrations, with low selectivity in biological samples and applications of several derivatization steps. These limitations are an obstacle to postmarketing pharmaceutical surveillance, especially of biological samples. Therefore, precise, rapid, and simple analytical tools are needed.

Electroanalytical measurements have been encouraged for quality control and monitoring of pharmaceutical residues based on their adequate sensitivity and simplicity of equipment compared with spectrometric and chromatographic techniques.[25−27] Electroanalytical approaches offer an advanced blend of simplicity while maintaining the sensitivity of the method by leveraging miniaturization and modifications of the active working electrodes. Electrochemical sensors are based on a selected recognition "sensing" element that "senses" and interacts with the target analyte and transducer that converts such interaction to a measurable electrical signal, which in turn is proportional to the target analyte concentration.[28] Voltammetric analysis offers many advantages due to the high sensitivity with the limit of detection in the subnanomolar levels and the possibility of simultaneous multianalyte measurement.[29] In this regard, carbon paste electrodes integrated with graphene nanosheets (NG/CPEs) were reported for the voltammetric determination of TAP in pharmaceutical samples within a linear concentration in the range from 17 to 136.3 ng mL^{-1}.[30]

As drug usage continues to rise, the adoption of screen-printed technology presents an opportunity to develop reliable portable devices. These devices can ensure strict safety compliance, facilitate urgent clinical assessments, and enable real-time monitoring of drug overdosages in a noninvasive manner, thereby curbing misuse and aiding law enforcement applications.[27,31] Screen-printed technology is a well-established and cost-effective technology that integrates reference, counter, and working electrodes onto a single substrate surface.[32] Such electrodes offer several additional advantages, including mass production with high selectivity, rapid detection, on-site applicability, real-time monitoring, and adaptability.[33]

To modify homemade screen-printed or carbon paste electrodes with a desired material, the most common approach is the use of drop casting in which a suitable aliquot of liquid containing a modifier suspension is deposited onto the electrode surface, and after evaporation of the solvent, a layer of the modifier was deposited on the electrode surface.[34] If done incorrectly, the distribution of the modifier across the surface is altered, which has a negative influence on the electroanalytical behavior of the modified sensor with poor stability. To circumvent the above limitations, an alternative modification approach can be recommended through fortification of the printing ink with the desired material, which reduces the resistance between the desired material and the electrode surface and improves electron transfer properties. Bulk modification provides a simple and effective approach, allowing one to create mass-produced electrochemical platforms. Recently, there has been a significant focus on tailor-made electrochemical sensors with improved performance via integration of the electrode matrices with various nanomaterials with a reported electrocatalytic activity, which facilitates the electrooxidation of the target analyte and electron transferee process at the electrode surface.[35−38] With promising electrocatalytic futures, CuONPs-based voltammetric sensors were encouraged for monitoring of various pharmaceutical compounds in their formulations and complex biological samples.[39−42]

In the present work, homemade planner screen-printed sensors bulk modified with CuONPs were developed for the voltammetric quantification of tapentadol. The sensor performance was evaluated for the linearity parameters, limit of quantification (LOQ), and detection and their selectivity against possible interference. The introduced sensors showed potential applications in pharmaceutical quality control and in vitro dissolution studies of TAP in commercial pharmaceutical formulations. As a sensitive disposable sensor, it can facilitate rapid drug screening and on-site detection, enabling early medical intervention in drug abuse cases.

2. EXPERIMENTAL SECTION

2.1. Tapentadol Authentic Sample and Chemical Reagents. Tapentadol hydrochloride standard sample (TAP-HCl, 3-((1*R*,2*R*)-3-(dimethylamino)-1-ethyl-2-methyl-propyl) phenol hydrochloride, $C_{14}H_{24}ClNO$, 99.90%, 175591-09-9) was purchased from Beijing Huikang Boyuan Chemical Tech Co., Ltd (China). The TAP solution was prepared by dissolving a precalculated amount of the TAP standard sample in deionized water. Graphite powder (1−2 μm, Aldrich) was applied for manufacturing a printing carbon ink. Various metal oxide nanostructures were implanted as modifiers, including copper oxide (Alfa Aesar), titanium oxide, iron oxide, and zinc oxide nanopowders supplied by Sigma-Aldrich. The drug-free biological fluids (VACSERA, Giza, Egypt) were applied as biological samples. The Britton−Robinson buffer solution (4×10^{-2} mol L^{-1}) was used, and the required pH was adjusted using the NaOH solution. Potassium ferricyanide (FCN, Sigma-Aldrich) was used for electrochemical impedance spectroscopic and surface area measurements.

2.2. Instrumentation and Construction of the Working Electrode. Metrohm workstation (797 VA, Switzerland) was applied for the voltammetric measurement connected with a three-electrode measuring cell containing Ag/AgCl as a reference electrode, the fabricated printed sensors as an active working electrode, and Pt wire as an auxiliary electrode. The conductive printing ink was formulated as described in detail elsewhere[43,44] by intimate mixing 0.5 g of graphite powder with 0.6 g of commercial nail polish. One gram portion of the homogeneous ink was enriched with 50 mg of the electrode modifier with continuous stirring. Carbon-based printing ink was printed onto an overhead projector PVC sheet with dimensions of 5 mm × 35 mm.[45,46] After curing for 2 h at 50 °C, individual printed sensors were covered with a protective layer of nail polish, leaving a circular working area of 3 mm diameter.

2.3. Recommended Analysis Protocol. The supporting electrolyte containing 15 mL of the BR buffer solution at pH 5 was enriched with suitable aliquots of the TAP standard

https://doi.org/10.1021/acsomega.4c09110
ACS Omega 2025, 10, 2897−2907

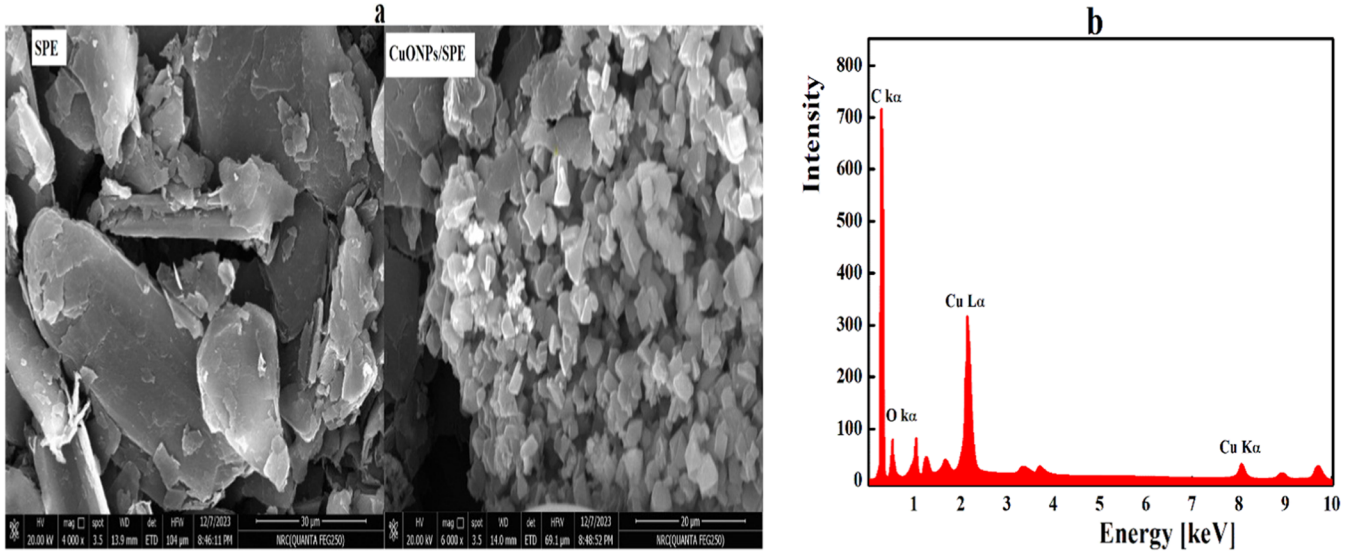

Figure 1. (a) SEM and (b) EDX of the fabricated CuONPs/SPEs.

solution. Differential pulse voltammograms were monitored under the following electroanalytical conditions: deposition potential of 0.1 V, accumulation time of 100 s, pulse amplitude of 50 mV, pulse width of 100 ms, pulse duration of 40 ms, scan rate of 44 mV s^{-1}, voltage step of 7 mV, and voltage step time of 0.15 s.

2.4. Analysis of the TAP Pharmaceutical and Biological Samples. The marketed tapentadol sample (Supratadol 100 mg of TAP-HCl/Tab, Pioneer Pharm. Industries, New Cairo, Cairo, Egypt) was collected from local drug stores. Five tablets were carefully ground, and weight equivalent to one tablet was dissolved in 40 mL of water and sonicated for 30 min. The sample solution was filtered, and the volume was adjusted to 50 mL with water. The sample solution was further diluted to an appropriate concentration, and the TAP content was measured at the optimized voltammetric conditions and spectrophotometrically at 280 nm.[21]

The standard plasma samples were spiked with suitable aliquots of the authentic TAP solution and mixed with acetonitrile (1:3 ratio). After centrifugation to precipitate the sample protein, the TAP content was analyzed voltammetrically and according to the spectrophotometric protocol. Similarly, the urine samples were spiked with TAP, followed by methanol and centrifugation to remove protein.

2.5. Measuring the Electroactive Surface Area (EASA). To estimate the electroactive surface area (EASA), successive cyclic voltammograms were recorded in the FCN solution at different scan rate values. The peak current was plotted versus the corresponding square root of the scan rate ($v^{1/2}$) values, and the EASA was calculated based on the Randles−Ševčík equation[47,48]

$$I_p = (2.99 \times 10^5) n^{3/2} A D^{1/2} C v^{1/2} \quad (1)$$

where n is the number of electrons transferred in the electrode reaction, A is the EASA, D is the diffusion coefficient (7.6×10^{-6} cm^2 s^{-1}), and C is the potassium ferricyanide concentration.

2.6. Stress Degradation of Tapentadol. The forced degradation studies of TAP were carried out following the ICH guidelines under different stress conditions including hydrolysis, oxidative degradation, thermal, and photolytic degradation.[49,50] For the acidic, basic, and neutral hydrolysis conditions, the TAP solution (1.0 mg mL^{-1}) was refluxed with HCl, NaOH, or water for 5 days at 80 °C. Under oxidative degradation conditions, the TAP sample was mixed with 5% H_2O_2 solution and incubated for 15 days at 25 °C. Thermal degradation study was tested on the solid TAP sample at 100 °C for 48 h. Under photolytic degradation, the solid TAP powder was exposed to UV light (360 Wh/m^{-2}) in the photostability chamber. After different intervals, samples of the degradation mixture were withdrawn and diluted to a suitable TAP concentration, and the absorbance was measured at 280 nm compared with the voltammetric measurements under the present procedure.

2.7. Dissolution Testing of the Tapentadol Pharmaceutical Sample. The dissolution profile of the commercial tapentadol pharmaceutical sample (Supratadol, 100 mg/tablet) was tested using USP apparatus type 1 in 900 mL of the HCl solution (0.1 N) as the dissolution medium at 37 °C and rotation speed of 75 rpm.[23] Definite aliquots were withdrawn from the dissolution media after different time intervals, and the released TAP was analyzed by the developed voltammetric approach in comparison to the spectrophotometric one.[51]

3. RESULTS AND DISCUSSION

3.1. Characterization of the CuONPs/SPCEs. As a newly formulated printing ink, the shape and morphology of the constructed sensors fortified with CuONPs were investigated with scanning electron microscopy (SEM) and energy-dispersive X-ray spectroscopy (EDX). SEM was utilized to assess the surface properties of modified CuONPs/SPE in contrast to unmodified printed sensors (Figure 1). For the blank printing ink, uniform and smooth graphite flakes with distinct layers were presented. In contrast, the emergence of relatively uniform CuONPs, with an average length of 35 nm bonded with carbon nanoparticles, exhibits a morphology resembling nanoparticles with nanoscale dimensions. These structures contribute to an augmented active surface area, while the presence of porosity and cave-like shapes enhances the electrode's geometry.

Additionally, EDX analysis reveals the uniform distribution of three main elements, such as C, O, and Cu, throughout the

https://doi.org/10.1021/acsomega.4c09110
ACS Omega 2025, 10, 2897−2907

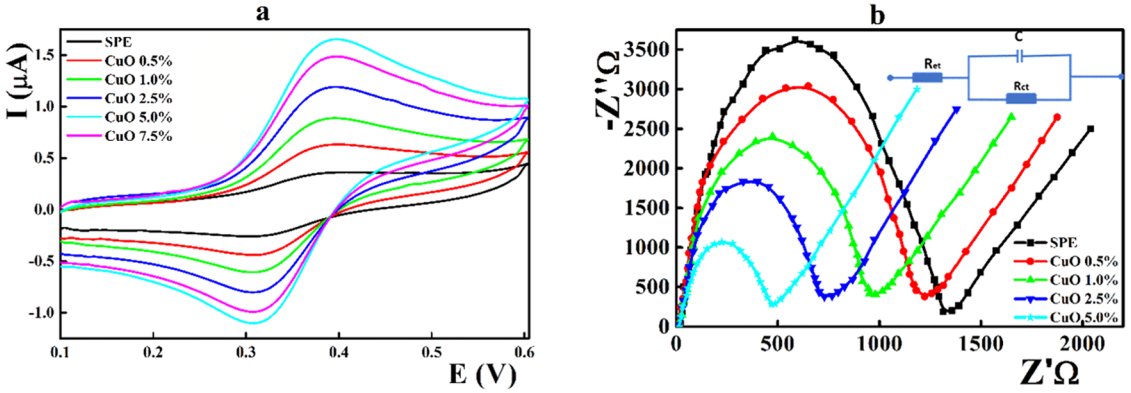

Figure 2. (a) Cyclic voltammograms and (b) EIS of the CuONPs/SPCEs recorded in 1.0×10^{-3} mol L^{-1} $K_4Fe(CN)_6$/0.1 mol L^{-1} KCl solution.

Table 1. Characteristics of the Anodic and Cathodic Peaks and the Electroactive Surface Area for Copper Nanoparticle Integrated Sensors Recorded in Potassium Ferricyanide Solution

electrode	E_{pa} (V)[a]	E_{pc} (V)	ΔE (V)	I_{pa} (μA)[b]	I_{pc} (μA)	I_{pa}/I_{pc}	electroactive surface area (cm^2)
SPE	0.386	0.314	0.072	0.133 ± 0.012	−0.123 ± 0.011	1.08	0.042 ± 0.009
CuONPs 0.5%	0.386	0.314	0.072	0.339 ± 0.022	−0.397 ± 0.016	0.85	0.063 ± 0.011
CuONPs 1.0%	0.386	0.314	0.072	0.526 ± 0.019	−0.598 ± 0.02	0.88	0.097 ± 0.014
CuONPs 2.5%	0.386	0.314	0.072	0.708 ± 0.017	−0.906 ± 0.013	0.78	0.127 ± 0.018
CuONPs 5.0%	0.392	0.314	0.078	1.090 ± 0.020	−1.130 ± 0.017	0.96	0.212 ± 0.020
CuONPs 7.5%	0.386	0.314	0.072	0.962 ± 0.018	−0.991 ± 0.012	0.971	0.221 ± 0.021

[a]The electrode potential was measured versus Ag/AgCl/3 M KCl as a reference electrode. [b]SD for three tropical measurements.

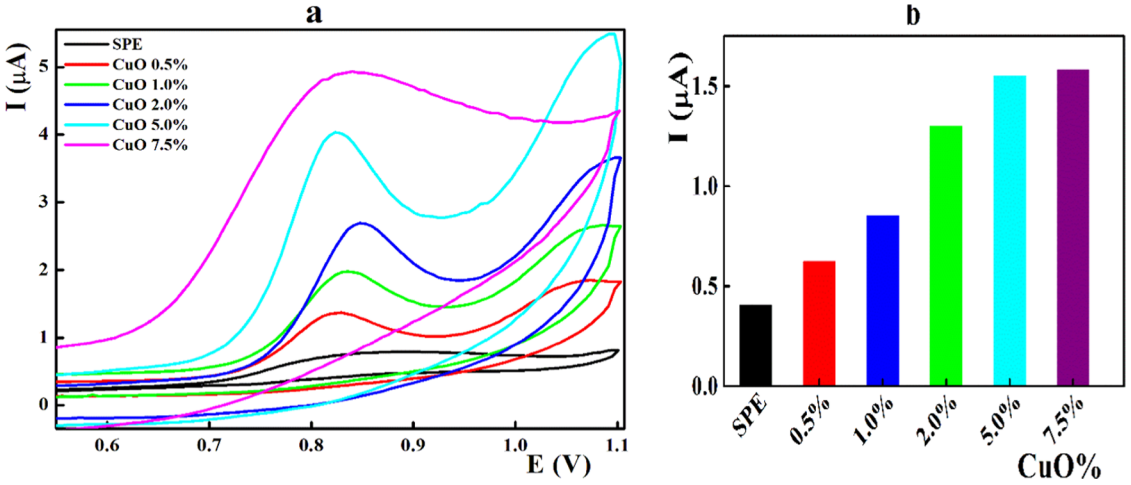

Figure 3. (a) Cyclic voltammetric determination of 4.0 μg mL^{-1} TAP at screen-printed carbon sensors incorporated with different CuONPs ratios and (b) peak current values recorded at different electrodes. Applied pH 5.0 and scan rate 0.044 V s^{-1}.

printing ink formulation (Figure 1b). The atomic weight percentages obtained from the EDX analysis indicate the presence of 5.2% Cu, 10.28% oxygen, and 82.95% carbon, confirming the homogeneous distribution of the nanocomposite.

Next, the electrochemical behavior of the printed sensors incorporated with different CuONP ratios was recorded in a ferricyanide solution (Figures 2, S1 and Table 1). The peak current values were reported to be improved via the incorporation of copper oxide nanoparticles. Even at a small modifier content (0.5%), the recorded anodic and cathodic peak current values were amplified by 2.55% compared to those of the bare electrode. Furthermore, a gradual increase of the peak current was reported at a higher CuONP content with a maximum value of 5.0%, which can be explained on the basis of enhanced electroactive surface area due to the presence of the metal oxide nanostructure within the electrode matrix.

Based on the Randles−Sevik equation described in Section 2.5, the EASA was estimated and is tabulated in Table 1. Gradual increase in the EASA was recorded upon modification with CuONPs with about 5-fold increase at a 5.0% modifier content compared with the blank electrode matrix.

Electrochemical impedance spectroscopy (EIS) was applied as an efficient electroanalytical tool to demonstrate the alteration at the electrode surface due to modification of the electrode matrix with the CuONPs. The Nyquist plots of the constructed sensors containing different concentrations of copper oxide nanostructures demonstrate the high capability of the modified sensors for following the charge across the measuring circuit (Figure 2b). Two different regions were

https://doi.org/10.1021/acsomega.4c09110
ACS Omega 2025, 10, 2897−2907

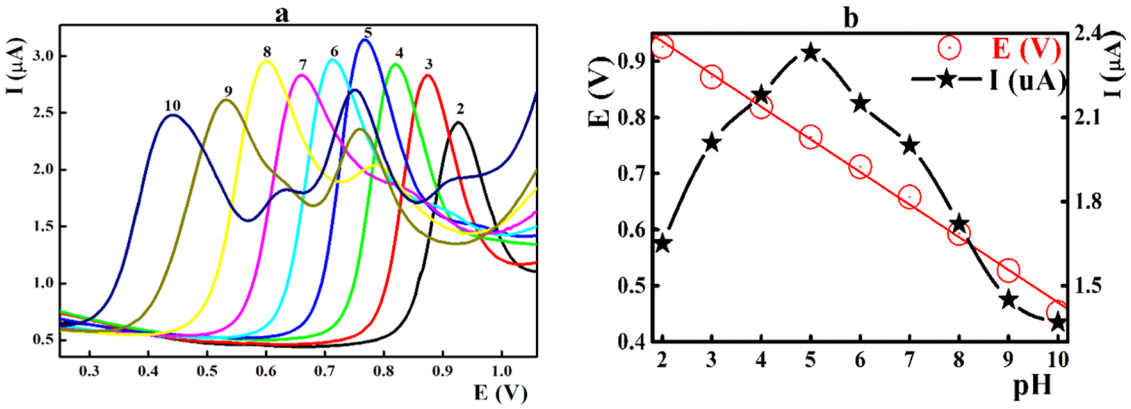

Figure 4. (a) DPVs recorded for 4.0 μg mL^{-1} TAP at different pH values. (b) Peak potential and current versus the pH value.

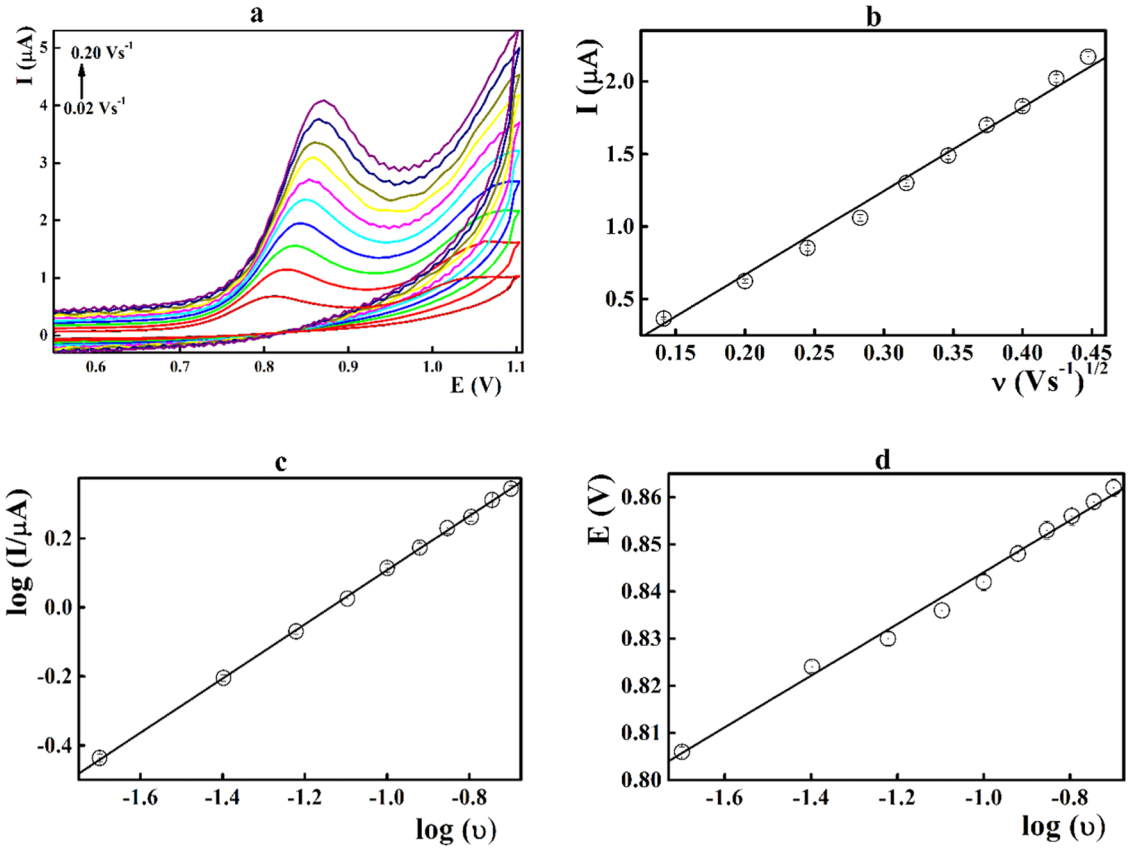

Figure 5. (a) Cyclic voltammograms recorded in the presence of 2.0 μg mL^{-1} TAP at pH 5 applying different scan rate values. (b) Peak current against the square root of the scan rate. (c) Logarithmic value of the peak current versus the logarithmic value of the scan rate. (d) Oxidation potential versus the logarithmic value of the scan rate.

presented: high-frequency regions (the first semicircle part), which refer to the electron transfer process, and low-frequency regions (linear part), which refer to the controlled diffusion processes at the electrode surface. Generally, the small radius of the semicircle part indicates the small resistance of the interface layer, which improves the charge transfer at the electrode surface.[52,53] Herein, the charge-transfer resistance (R_{ct}) values were found to be equal to 1290, 1158, 905, 725, and 472 Ω, related to different ratios of CuONPs. The incorporation of 5.0% CuONPs indicated the lowest R_{ct} value with excellent electrical conductivity.

3.2. Voltammetric Behavior of Tapentadol at CuONP-Based Sensors. At graphene nanosheet integrated carbon paste electrodes (NG/CPEs),[30] TAP molecules recorded an irreversible oxidation peak at about 0.92 V. Based on their electrocatalytic activity, various metal oxide nanostructures were recommended as electrode modifiers for advanced analysis opportunities and enhanced sensor performance. Enhancement of the electron transfer kinetics and shifting of the oxidation peak potential toward the cathodic direction were reported. Therefore, the present study was devoted to exploring the oxidation behavior of TAP at the fabricated CuONPs/SPEs (Figure 3). On the bare SPEs, TAP recorded a broad irreversible anodic peak at 0.840 V. Enhancement of the peak current with continuous shifting of the peak potential toward the cathodic direction (by about 30 mV) upon

https://doi.org/10.1021/acsomega.4c09110
ACS Omega 2025, 10, 2897−2907

modification with copper oxide nanostructure was reported. This improvement of the electrode performance may be explained based on the existence of Cu(III)/Cu(II) transition redox couples, which facilitates the oxidation of the TAP at the CuONPs/SPEs surface.[54]

To attain the proper performance of the fabricated sensors, different amounts of CuONPs were added to the printing ink matrix (Figure 3b). The current values gradually increased to reach a maximum value at 5.0% CuONPs. At higher ratios of CuONPs, a broad oxidation peak with a higher background current was recorded, which may be due to the high conductivity of the formulated printing ink; therefore, 5.0% CuONPs was the proper content.

At the optimum electrode matrix composition, the CuONPs were replaced by other metal oxide nanostructures (Figure S2). Copper oxide exhibited the highest electrocatalytic effect based on the variation of band gaps and redox potentials of the tested oxide forms.[54]

3.3. Effect of pH of the Supporting Electrolyte. Tapentadol showed two pK_a values of 9.34, corresponding to the tertiary amine group, and 10.45, related to the phenolic group.[12] Therefore, the impact of the pH of the supporting electrolyte was tested within the pH range of 2−10 (Figure 4a). The potential values were shifted toward the cathodic direction at higher pH values, indicating the participation of protons in the oxidation of TAP at the electrode surface.[55−57] Meanwhile, sharp and distinct differential pulse peaks were monitored at lower pH values (2−6), the main peak became broad, at higher pH values, and a new peak appeared at 0.747 V. Plotting the peak potential against the pH value revealed a linear relationship with an ideal theoretical Nernstian slope value, demonstrating the transfer of an equal number of protons/electrons in the electrode reaction [$E_{(V)}$ = 1.052−0.058 ± 0.001, [pH], r = −0.9981, Figure 4b]. Among the different tested pH values, pH 5 was selected as the proper pH with the highest peak current.

3.4. Electrochemical Behavior of Tapentadol at Different Scan Rates. Studying the electrochemical behavior at different scan rates explains the electrode reaction mechanism and estimates the number of electrons transferred.[55−57] Within the studied can rate value, TAP exhibited a single oxidation peak (Figure 5a). The peak current was improved at higher scan rate values, while the peak potential was shifted from 0.806 V at a scan rate of 0.02 V s^{-1} to about 0.877 V at 0.20 V s^{-1}. The current values were linearly correlated (r = 0.9959, Figure 5b) against the square root of the scan rate, sustaining the irreversibility of the electrode reaction.

Figure 5c illustrates the linear relationship between the logarithmic values of the peak current against the logarithmic values of the scan rate [$\log I_{(\mu A)}$ = 0.8949 + 0.7865 ± 0.005 [$\log(\upsilon)$], r = 0.9998]. The slope value suggested an adsorption-controlled mechanism for TAP at the CuONPs/SPEs,[56,57] which disagrees with that reported for TAP at the graphene-based carbon paste electrode.[30]

The oxidation potential of TAP was shifted to a more positive value following a linear dependence on the applied scan rate (υ) value [$E_{(V)}$ = 0.8990 + 0.0549 ± 0.0016 $\log(\upsilon)$, r = 0.9966, Figure 5d]. Following the Laviron equation for irreversible electrode reactions,[58] the number of electrons can be estimated as follows

$$E_{pc} = E^0 + \frac{RT}{\alpha nF}\ln\left(\frac{RTk^0}{\alpha nF\nu}\right) \quad (2)$$

where E_{pc} is the peak potential, E^0 is the standard redox potential, R is the universal gas constant, T is the temperature, α is the transfer coefficient, n is the number of electrons transferred, F is the Faraday constant, k^0 is the standard rate constant, and ν is the scan rate.

Based on the slope value of the E_p versus $\log \upsilon$, αn can be estimated to be 1.0769, where the value of α can be calculated according to the following formula

$$\alpha = \frac{47.7}{E_p - E_{1/2}} \quad (3)$$

$E_{1/2}$ (mV) indicated the peak potential at which the peak current is half its maximum (Figure S3). The value of α was found to equal 0.5360, assuming the participation of two electrons during the oxidation of the TAP at the electrode surface. The apparent heterogeneous electron transfer rate constant (κ_s) was calculated ($\kappa_s = \alpha nF\nu/RT$) and found to equal 2.08 × 10^{-4} s^{-1}.[48]

Alternately, the Tafel plot region equation can be applied to calculate the number of electrons participating according to ref 59

$$\eta = a + b\log(i) \quad (4)$$

where η is the overpotential, a is the Tafel constant (intercept), b is the Tafel slope, and i is the current density.

As illustrated in Figure S4, the peak potential (V) showed a linear relationship against the logarithmic value of the peak current [$E_{(V)}$ = 1.5878 + 0.1347 $\log I(\mu A)$; r^2 = 0.9984]. The Tafel slope [$2.303RT/[(1-\alpha)\ \alpha nF]$] postulated the value of α = 0.690, which approximately agreed with that estimated based on the Laviron equation.

The influence of the deposition potential and time on the peak current was studied (Figure S5). The recorded peak current increased against the deposition potential with a maximum value at 0.1 V. No noticeable enhancement was achieved at a more positive deposition potential. Applying a deposition potential value of 0.1 V, the accumulation time varied from 0 to 200 s, and the accumulation for 100 s was the most proper.

It is noteworthy to mention that the experimental design approach would have been better than a one-factor-at-a-time one in the present study and will be included in the future investigations.

The reported results concerning the voltammetric behavior of TAP at different pH values and scan rate values with the aid of molecular orbital calculations (MOCs) were integrated to elucidate a primary oxidation mechanism for TAP at the CuONPs/SPE surface.[60] MOC is presented in Figure S6 and Table S1, suggesting that the highest electron density at nitrogen atom of the tertiary amine group (N7) with unlocalized lone pairs of electrons possesses more basic nature compared to the oxygen atom at position 13 (Scheme 1). This proposed oxidation mechanism of the TAP molecule aligns with that reported at NG/CPE.[30]

3.5. Validation of the CuONPs/SPEs. The electroanalytical performance of the newly tapentadol sensors based on copper oxide nanoparticles was validated under the selected optimal electroanalytical conditions.[61] The supporting electrolyte at pH 5 was spiked with selected increments of the

https://doi.org/10.1021/acsomega.4c09110
ACS Omega 2025, 10, 2897−2907

Scheme 1. Tentative Electrochemical Oxidation Mechanism of Tapentadol at CuONPs/SPCEs at pH 5

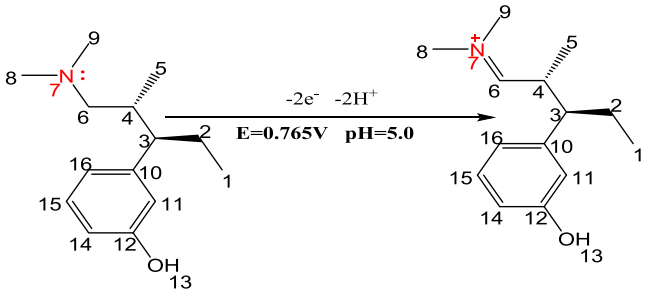

standard TAP solution, and the DPVs were recorded at the optimized electroanalytical parameters (Figure 6). The

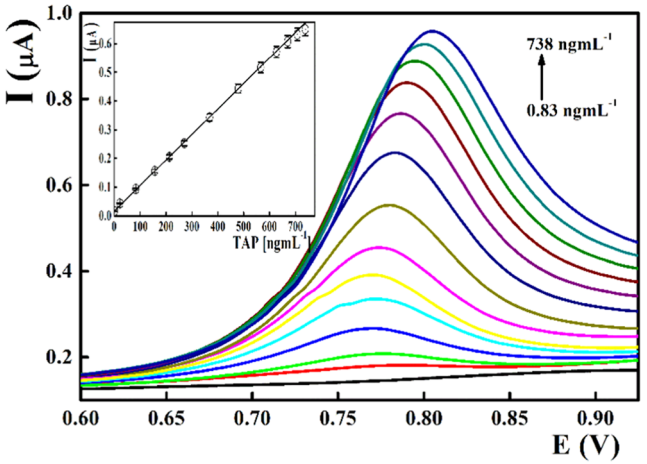

Figure 6. Differential pulse voltammetric determination of tapentadol at CuONPs/SPEs recorded at pH 5 and a scan rate of 0.044 V s^{-1}.

constructed calibration graphs showed a high linearity coefficient (r^2 = 0.9995) within the TAP concentration ranging from 0.83 to 738 ng mL^{-1} (Table 2). Based on the linearity parameters, the limit of quantification (LOQ) and limit of detection (LOD) values were 0.80 and 0.24 ng mL^{-1}, respectively.

To evaluate the measurement reproducibility of the CuONPs/SPCEs, successive DPVs were recorded at the same electrode surface; after each cycle, the electrode surface was washed with water (Figure S7). The recorded peak current showed high reproducibility with a low RSD value (1.53%). One of the most promising futures of screen printing technology is the mass production of simple planar configuration disposable sensors with the maintenance of high fabrication reproducibility. Herein, the reproducibility of manual screen printing of electrodes was evaluated by testing 10 printed sensors within the same batch for differential pulse voltammetric measurement of a 500 ng mL^{-1} tapentadol solution (three replicates for each electrode). The estimated RSD value was 3.75%, indicating the high fabrication reproducibility of the printed sensors.

Table 2. Validation and Electroanalytical Performance of Tapentadol CuONPs/SPEs

parameters	value[a]
peak potential	0.765 V
pH value	5
concentration range (ng mL^{-1})	0.83−738
slope (μA mL^{-1} ng^{-1})	0.0010
SD_{slope} (μA mL^{-1} ng^{-1})	0.0009
intercept (μA cm^{-2})	0.0022
$SD_{intercept}$ (μA cm^{-2})	0.0021
R^2	0.9995
RSD %	1.53
LOQ (ng mL^{-1})	0.80
LOD (ng mL^{-1})	0.24

[a]Average of five experiments.

The solid nature and the absence of the pasting liquid of the fabricated sensors prolonged their shelf lifetime when stored at 4 °C. In this study, the sensor performance was tested periodically at the storage period of 6 months (Figure S8). Reproducible voltammetric peaks were recorded during the first three months (96.34 ± 1.8% of the initial peak current for the freshly printed sensor was recorded after 3 months). Later, the peak height was diminished to 94.69 ± 2.2% of the original value after 4 months and decreased to 86.04 ± 2.8% after 6 months of storage.

Compared with the NG/CPEs TAP voltammetric sensor,[30] the CuONPs/SPCEs showed improved sensitivity covering a wide TAP concentration range with a lower LOD value (Table S2). In addition, the high manufacturing reproducibility and possibility of miniaturization with a prolonged shelf lifetime represent the main advantage of the presented sensors.

3.6. Selectivity of the Sensor. Impurities degradation profiling of the pharmaceutically active compound that present in the final marketed pharmaceutical product and dealing with the quantifying and studying the residual manufacturing impurities and the possible degradation products that formed during storage of the final pharmaceutical formulations. Identification and detection of such contaminants and degradation products represent a crucial consideration in the pharmaceutical industry. Thus, the developed analytical approaches must be able to detect the parent pharmaceutically active compounds in the presence of various impurities and degradants to ensure the safety of the marketed pharmaceutical product.[49,,63]

Degradation and stability studies are crucial issues for the approval of a new pharmaceutical product to ensure quality, efficacy, and safety during its shelf life.[63−6465] In this study, TAP showed intrinsic stability under acidic, basic, or neutral hydrolysis conditions. Exposure of a solid TAP sample to thermal or photolytic conditions showed negligible degradation percentages.[13,49] Under oxidative conditions, two degradation products were produced through the oxidation of the tertiary amine group forming N-oxide-TAP and oxidation of the carbon atom (C3) within the TAP moiety.[49,66] Regarding the voltammetric behavior of the degraded form, none of the two degradation products showed oxidation peaks due to the involvement of the unlocalized lone pairs of electrons of the nitrogen atom forming N-oxide oxide−TAP. The presented results indicate the absence of interference of the two TAP degradation products; therefore, the fabricated sensor can be introduced as a stability-indicating method for monitoring TAP in pharmaceutical formulations.

Moreover, the impact of different excipients or additives that may be present in the final formulation was tested by recording the DPVs for 500 ng mL^{-1} TAP in the presence of these interferents. High tolerance limits were recorded in the

https://doi.org/10.1021/acsomega.4c09110
ACS Omega 2025, 10, 2897−2907

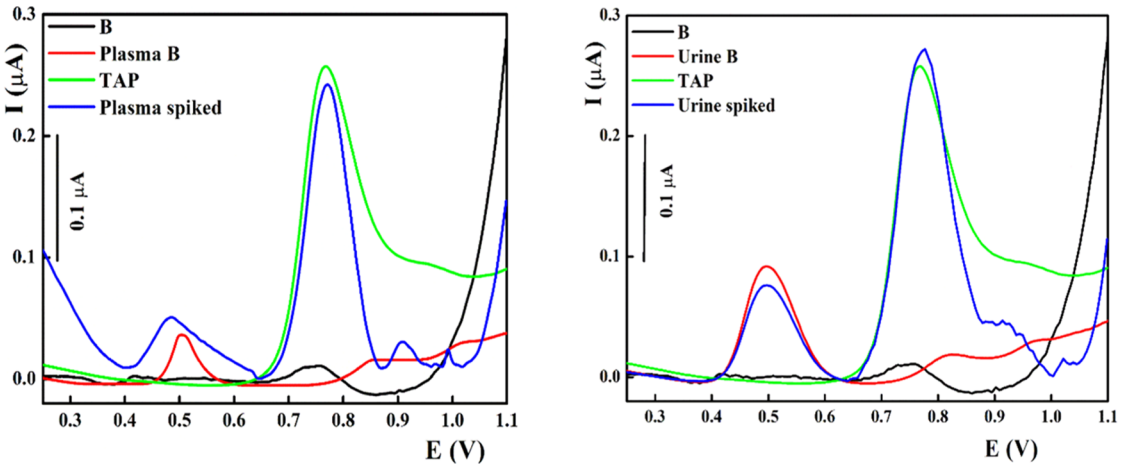

Figure 7. Differential pulse voltammetric determination of TAP in spiked biological samples using CuONPs/SPEs at pH 5.0. TAP (300 ng mL^{-1}).

presence of a 100-fold of the interferents. For pain treatment, tapentadol is usually co-formulated or administrated with paracetamol (PC). Some previous studies were carried out for simultaneous determination of TAP and PC by applying spectrophotometric and chromatographic approaches.[20,21,46] Therefore, this study investigated the possibility of simultaneous calibration of both PC and TAP on CuONPs/SPEs (Figure S9). Two separate and distinct oxidation peaks were recorded at 0.450 and 0.770 V, allowing simultaneous determination of both compounds. Within the PC concentration ranged from 20 to 500 ng mL^{-1}, the linear regression equation was $I_{(\mu A)}$ = 0.9720 + 0.0091 PC [ng mL^{-1}] (r = 0.99577). In addition, TAP showed a good linear coefficient (r = 0.9994) within the concentration range from 50 to 700 ng mL^{-1} ($I_{(\mu A)}$ = 0.0945 + 0.00098 TAP [ng mL^{-1}]).

Electrochemical interactions between TAP, uric acid (UA), and ascorbic acid (AA) represent a challenge due to their coexistence in biological samples. The interference of AA with TAP detection arises from two main factors: the close oxidation potentials of AA and TAP (0.400 and 0.780 V, respectively) and the electrocatalytic oxidation of TAP by AA. At the fabricated CuONPs/SPE in BR buffer (pH = 5), various interactions affect the oxidation of AA and TAP takes place. The voltammetric response of ascorbate anions at the electrode surface suggests electrostatic interactions between ascorbate anions and cationic-fixed sites at the electrode surface. Meanwhile, the positively charged amino group of the TAP moiety at pH = 5.0 experiences electrostatic repulsion from the electrode surface in the BR buffer solution, resulting in slow catalytic effects toward TAP molecules. Surprisingly, in our study, copper oxide nanoparticles did not hinder the electrochemical oxidation of TAP, yielding a relatively higher current signal. This unexpected outcome can be explained based on the compensatory effect of hydrophobic interaction between the aromatic part of TAP and the electrode surface. It is plausible that the aromatic portion of TAP engaged in hydrophobic interaction with the electrode surface while its cationic part protruded outward. This unique behavior sheds light on the intricate interplay between TAP and the electrode surface, contributing to our understanding of electrochemical processes involving complex organic molecules. It can be concluded that the simultaneous measuring of TAP, AA, and UA can be performed using the fabricated CuONPs/SPE (Figure S10) if PC is not present in the biological fluids under analysis.

3.7. Dissolution Studies. Absorption of the pharmaceutically active ingredient after oral administration represents an important consideration to confirm the pharmacokinetics behavior of the drug and the release of the pharmaceutically active component from the drug formulations. Moreover, the in-dissolution studies are usually relevant to predict the in vivo bioavailability of the drug product and help in suggesting a new formulation with a faster or slower release rate according to the use of the pharmaceutical product, which ensures product optimization as well as continuing product quality and performance of the manufacturing process.

For testing the dissolution profile of TAP in its commercial form (Supratadol tablet), the released amount of TAP in the dissolution medium was monitored spectrophotometrically at 280 nm according to the presented voltammetric sensor. Results illustrated in Figure S11 indicate approximate recovery values obtained by UV and voltammetric approaches (±2.0%). As a result, TAP showed a rapid release rate (about 70% was released within 30 min), and more than 90% was achieved within 50 min. Thus, the developed sensor can be suggested for monitoring the dissolution of the tapentadol pharmaceutical formulation.

3.8. Analysis of the Sample. The fabricated CuONPs/SPE showed high selectivity and sensitivity toward tapentadol; therefore, they can be applied for the determination of TAP in marketed pharmaceutical products and biological samples (Figure 7). The recorded data indicated high recovery with low standard deviation values; therefore, the CuONPs/SPEs can be encouraged for quality control of tapentadol in its pharmaceutical tablets and biological samples (Tables S3 and S4).

4. CONCLUSIONS

Fabrication and characterization of a planar disposable carbon sensor modified with copper oxide nanoparticles were described for the selective and sensitive voltammetric determination of tapentadol in pharmaceutical and biological samples. Enrichment of the printing ink matrix with copper oxide nanoparticles improved the sensor performance based on its electrochemical activity toward the oxidation of TAP at pH 5 with an adsorption-controlled mechanism. The constructed sensors showed high measurement and fabrication reproduci-

https://doi.org/10.1021/acsomega.4c09110
ACS Omega 2025, 10, 2897−2907

bility with a prolonged shelf lifetime of up to 6 months. The introduced analytical approach can be suggested as a stability-indicating method free from the interference of TAP degradation products. The CuONPs/SPEs voltammetric sensor can be considered a reliable analytical approach for sensitive quantification of tapentadol as well as monitoring the in vitro dissolution profile of the pharmaceutical formulation.

■ ASSOCIATED CONTENT

Data Availability Statement

All data generated or analyzed during this study are included in the article (and the Supporting Information).

Supporting Information

The Supporting Information is available free of charge at https://pubs.acs.org/doi/10.1021/acsomega.4c09110.

Peak current for anodic and cathodic peaks of the recorded cyclic voltammograms and electroactive surface area of the fabricated sensors. The measuring solution contained 1.0×10^{-3} mol L^{-1} $K_4Fe(CN)_6$/0.1 mol L^{-1} KCl (Figure S1). Cyclic voltammograms recorded for screen-printed carbon sensors incorporated with different metal oxide nanostructures. Measuring conditions. TAP content 4.0 μg mL^{-1}, applied pH 5.0, and scan rate 0.044 V s^{-1} (Figure S2). Estimation of the E_p and $E_{1/2}$ of the TAP according to the EC-Lab V10.40 software (Figure S3). Tafel region plot for oxidation of 2.0 μg mL^{-1} tapentadol (pH 5) at the CuONPs/SPCEs. Inset: related linear sweep voltammogram at a scan rate of 20 mV S^{-1} (Figure S4). Peak heights of the recorded DPV for 1.0 μg mL^{-1} tapentadol at applying different (a) deposition potential values and (b) depositions times (Figure S5). Chemical formula of tapentadol molecule (Figure S6). Successive DPVs were recorded for 500 ng mL^{-1} tapentadol at pH 5 applying the same CuONPs/SPEs surface (Figure S7). Differential pulse voltammograms for 500 ng mL^{-1} tapentadol at CuONPs/SPCEs after different shelf lifetime intervals (Figure S8). Simultaneous differential pulse voltammetric determination of PC and TAP using the CuONPs/SPEs at pH 5.0 (Figure S9). Simultaneous differential pulse voltammetric determination of TAP (750 ng mL^{-1}), AA (200 ng mL^{-1}), and UA (2 μg mL^{-1}) using the CuONPs/SPEs at pH 5.0 (Figure S10). Dissolution studies of tapentadol pharmaceutical formulation (Figure S11). Computed molecular orbital calculations of tapentadol molecule (Table S1). Comparison of different tapentadol sensors (Table S2). Assay of tapentadol in pharmaceutical formulations (Table S3). Assay of tapentadol in biological samples (Table S4) (PDF)

■ AUTHOR INFORMATION

Corresponding Author

Nashwa M. El-Metwaly − *Department of Chemistry, Faculty of Sciences, Umm Al-Qura University, Makkah 21955, Saudi Arabia; Department of Chemistry, Faculty of Science, Mansoura University, Mansoura 002050, Egypt;* orcid.org/0000-0002-0619-6206; Email: n_elmetwaly00@yahoo.com, nmmohamed@uqu.edu.sa

Authors

Razan M. Snari − *Department of Chemistry, Faculty of Sciences, Umm Al-Qura University, Makkah 21955, Saudi Arabia*

Zehbah A. Al-Ahmed − *Applied College Dhahran Aljanoub, King Khalid University, Abha 61421, Saudi Arabia*

Arwa Alharbi − *Department of Chemistry, Faculty of Sciences, Umm Al-Qura University, Makkah 21955, Saudi Arabia*

Abdullah A. A. Sari − *Department of Chemistry, University Collage in Al-Jamoum, Umm Al-Qura University, Makkah 21955, Saudi Arabia*

Hanadi A. Katouah − *Department of Chemistry, Faculty of Sciences, Umm Al-Qura University, Makkah 21955, Saudi Arabia*

Reem Shah − *Department of Chemistry, Faculty of Sciences, Umm Al-Qura University, Makkah 21955, Saudi Arabia*

Fawaz A. Saad − *Department of Chemistry, Faculty of Sciences, Umm Al-Qura University, Makkah 21955, Saudi Arabia*

Fathy Shaaban − *Department of Environment and Health Research, Umm Al-Qura University, Makkah 21955, Saudi Arabia*

Complete contact information is available at: https://pubs.acs.org/10.1021/acsomega.4c09110

Notes

The authors declare no competing financial interest.

■ ACKNOWLEDGMENTS

The funding is personal from the authors.

■ REFERENCES

(1) Kiedrowski, M. Tapentadol helps in trigeminal neuralgia: a case report. *Ann. Palliat. Med.* **2024**, *13*, 17882−17182.

(2) Jain, D.; Basniwal, P. K. Tapentadol, a novel analgesic: Review of recent trends in synthesis, related substances, analytical methods, pharmacodynamics and pharmacokinetics. *Bull. Fac. Pharm.* **2013**, *51*, 283−289, DOI: 10.1016/j.bfopcu.2013.04.003.

(3) O'Connor, J.; Christie, R.; Harris, E.; Penning, J.; McVicar, J. Tramadol and Tapentadol: Clinical and Pharmacologic Review. In *Anaesthesia Tutorial of the Week*, 2019; Vol. *407*, pp 1−6.

(4) Stollenwerk, A.; Sohns, M.; Heisig, F.; Elling, C.; von Zabern, D. Review of post-marketing safety data on tapentadol, a centrally acting analgesic. *Adv. Ther.* **2018**, *35*, 12−30.

(5) Deeks, E. D. Tapentadol prolonged release: a review in pain management. *Drugs* **2018**, *78*, 1805−1816.

(6) Tayal, G.; Grewal, A.; Mittal, R.; Bhatia, N. Tapentadol-a novel analgesic. *J. Anaesthesiol., Clin. Pharmacol.* **2009**, *25*, 463−466.

(7) Terlinden, R.; Ossig, J.; Fliegert, F.; Lange, C.; Göhler, K. Absorption, metabolism, and excretion of ^{14}C-labeled tapentadol HCl in healthy male subjects. *Eur. J. Drug Metab. Pharmacokinet.* **2007**, *32*, 163−169.

(8) Channell, J. S.; Schug, S. Toxicity of tapentadol: a systematic review. *Pain Manage.* **2018**, *8*, 327−339.

(9) Gevirtz, C. A. Comparative Analysis of Tapentadol, Tramadol, and the Opiates. *Top. Pain Manage.* **2010**, *25*, 1−7.

(10) Dyer, E. M.; Salehian, S. How to interpret urine toxicology tests. *Arch. Dis. Child. Educ. Pract. Ed.* **2020**, *105*, 84−88.

(11) Marathe, G. M.; Patil, P. O.; Patil, D. A.; Patil, G. B.; Bari, S. B. Stability indicating RP-HPLC method for the determination of tapentadol in bulk and in pharmaceutical dosage form. *Int. J. Chem. Technol. Res.* **2013**, *5*, 34−41.

(12) Jain, D.; Basniwal, P. K. ICH guideline practice: application of validated RP-HPLC-DAD method for determination of tapentadol hydrochloride in dosage form. *J. Anal. Sci. Technol.* **2013**, *4*, 1−7.

(13) Kathirvel, S.; Satyanarayana, S. V.; Devalarao, G. Application of a validated stability-indicating LC method for the simultaneous estimation of tapentadol and its process-related impurities in bulk and its dosage form. *J. Chem.* **2013**, *2013*, No. 927814.
(14) Kathirvel, S.; Madhu Babu, K. A validated method for the determination of tapentadol hydrochloride in bulk and its pharmaceutical formulation by densitometric analysis. *Indian Drugs* **2012**, *49*, 51.
(15) Kieves, N. R.; Howard, J.; Lerche, P.; Lakritz, J.; Aarnes, T. K. Effectiveness of tapentadol hydrochloride for treatment of orthopedic pain in dogs: a pilot study. *Can. Vet. J.* **2020**, *61*, 289.
(16) Hillewaert, V.; Pusecker, K.; Sips, L.; Verhaeghe, T.; de Vries, R.; Langhans, M.; Terlinden, R.; Timmerman, P. Determination of tapentadol and tapentadol-O-glucuronide in human serum samples by UPLC−MS/MS. *J. Chromatogr. B* **2015**, *981*−*982*, 40−47.
(17) Adluri, P.; Kumar, Y. S. Development and validation of stability indicating LC-MS/MS Technique for the quantification of tapentadol in biological matrices: Application to bioavailability study in healthy rabbits. *J. Appl. Pharm. Sci.* **2019**, *9*, 068−074.
(18) Mobrouk, M. M.; El-Fatatry, H. M.; Hammad, S. F.; Mohamed, A. A. Spectrophotometric Methods for Determination of Tapentadol Hydrochloride. *J. Appl. Pharm. Sci.* **2013**, *3*, 122−125.
(19) Ramadevi, U.; Madhavi, T.; Amruth Kumar, N.; Thiruvengada Rajan, V. S. Analytical Method Development and Validation of Tapentadol Hydrochloride in Tablet Formulation By UV Spectroscopic Method. *Int. J. Res. Pharm. Sci.* **2013**, *3* (2), 202−215.
(20) Joshi, C.; Mansuri, J.; Hariyani, H.; Gandhi, P.; Radadiya, R.; Faldu, D. S. Q-Absorbance ratio spectrophotometric method for the simultaneous estimation of Paracetamol and Tapentadol hydrochloride in bulk drug and in pharmaceutical dosage form. *Int. Bull. Drug Res.* **2013**, *3*, 37−45.
(21) El-Fatatry, H. M.; Mabrouk, M. M.; Hammad, S. F.; El-Malla, S. F. Simultaneous determination of tapentadol HCl and paracetamol by ratio-spectra derivative spectrophotometry. *World J. Pharm. Sci.* **2015**, 1290−1297.
(22) Dnbeel, N. N.; Al Abdali, Z. Z.; Omer, L. S.; Al-Sabha, T. N. Kinetic spectrophotometric determination of tapentadol. *MINAR Int. J. Appl. Sci. Technol.* **2023**, *5* (2), 41−58.
(23) Panikumar, D. A.; Haripriya, A.; Sirisha, N.; Venkat Raju, Y.; Sunitha, G.; Venkateswara Rao, A. Stability indicating spectrofluorimetric quantification of Tapentadol HCl and application to in-vitro dissolution studies. *J. Appl. Pharm.* **2013**, *5*, 794−804.
(24) Ganorkar, S. B.; Shirkhedkar, A. A. Design of experiments in liquid chromatography (HPLC) analysis of pharmaceuticals: Analytics, applications, implications and future prospects. *Rev. Anal. Chem.* **2017**, *36*, No. 20160025.
(25) Siddiqui, M. R.; AlOthman, Z. A.; Rahman, N. Analytical techniques in pharmaceutical analysis: A review. *Arab. J. Chem.* **2017**, *10*, S1409−S1421.
(26) Kurbanoglu, S.; Ozkan, S. A.; Merkoçi, A. Electrochemical Nanobiosensors in Pharmaceutical Analysis. *Novel Developments Pharm. Biomed. Anal.* **2018**, *2*, 302−353.
(27) Jadon, N.; Hosseinzadeh, B.; Kaya, S. I.; Ozcelikay-Akyildiz, G.; Cetinkaya, A.; Ozkan, S. A. Emerging trends of ion-selective electrodes in pharmaceutical applications. *Electrochim. Acta* **2024**, *488*, No. 144204.
(28) Ambaye, A. D.; Kefeni, K. K.; Mishra, S. B.; Nxumalo, E. N.; Ntsendwana, B. Recent developments in nanotechnology-based printing electrode systems for electrochemical sensors. *Talanta* **2021**, *225*, No. 121951.
(29) Kolesnichenko, I. Development of a Method for Multisensory Stripping Voltammetry in the Analysis of Medical Preparations. *ACS Omega* **2023**, *8*, 40229−40241.
(30) El-Shal, M. A.; Hendawy, H. A.; Eldin, G. M.; El-Sherif, Z. A. Application of nano graphene-modified electrode as an electrochemical sensor for determination of tapentadol in the presence of paracetamol. *J. Iran. Chem. Soc.* **2019**, *16*, 1123−1130.
(31) Teymourian, H.; Parrilla, M.; Sempionatto, J. R.; Montiel, N. F.; Barfidokht, A.; Van Echelpoel, R.; De Wael, K.; Wang, J. Wearable electrochemical sensors for the monitoring and screening of drugs. *ACS Sens.* **2020**, *5*, 2679−2700.
(32) Ferrari, A. G. M.; Rowley-Neale, S. J.; Banks, C. E. Screen-printed electrodes: Transitioning the laboratory in-to-the field. *Talanta Open* **2021**, *3*, No. 100032.
(33) Singh, S.; Wang, J.; Cinti, S. An overview on recent progress in screen-printed electroanalytical (bio) sensors. *ECS Sens. Plus* **2022**, *1*, No. 023401.
(34) Crapnell, R. D.; Banks, C. E. Electroanalytical Overview: Screen-Printed Electrochemical Sensing Platforms. *ChemElectroChem* **2024**, No. 202400370.
(35) Bozal-Palabiyik, B.; Erkmen, C.; Kurbanoglu, S.; Ozkan, S. A.; Uslu, B. Electrochemical analysis for pharmaceuticals by the advantages of metal oxide nanomaterials. *Curr. Anal. Chem.* **2021**, *17*, 1322−1339.
(36) Agnihotri, A. S.; Varghese, A.; Nidhin, M. Transition metal oxides in electrochemical and bio sensing: A state-of-art review. *Appl. Sur. Sci. Adv.* **2021**, *4*, No. 100072.
(37) Qian, L.; Durairaj, S.; Prins, S.; Chen, A. Nanomaterial-based electrochemical sensors and biosensors for the detection of pharmaceutical compounds. *Biosen. Bioelectron.* **2021**, *175*, No. 112836.
(38) Falola, T. O. Nanoparticles Modified Electrodes: Synthesis, Modification, and Characterization- Review. *World J. Nano Sci. Eng.* **2022**, *12*, 29−62.
(39) Maciulis, V.; Ramanaviciene, A.; Plikusiene, I. Recent Advances in Synthesis and Application of Metal Oxide Nanostructures in Chemical Sensors and Biosensors. *Nanomaterials* **2022**, *12*, 4413.
(40) Hendawy, H. A.; Khaled, E.; Radowan, A. Voltammetric determination of Marbofloxacin at carbon paste sensor integrated with copper oxide nanoparticles. *Electroanalysis* **2023**, *35*, No. e202200402.
(41) Boobphahom, S.; Ruecha, N.; Rodthongkum, N.; Chailapakul, O.; Remcho, V. T. A copper oxide-ionic liquid/reduced graphene oxide composite sensor enabled by digital dispensing: Non-enzymatic paper-based microfluidic determination of creatinine in human blood serum. *Anal. Chim. Acta* **2019**, *1083*, 110−118.
(42) Janmee, N.; Preechakasedkit, P.; Rodthongkum, N.; Chailapakul, O.; Potiyaraj, P.; Ruecha, N. A non-enzymatic disposable electrochemical sensor based on surface-modified screen-printed electrode CuO-IL/rGO nanocomposite for a single-step determination of glucose in human urine and electrolyte drinks. *Anal. Methods* **2021**, *13*, 2796−2803.
(43) Cândido, T. C.; Pereira, A. C.; da Silva, D. N. Development and Characterization of Conductive Ink Composed of Graphite and Carbon Black for Application in Printed Electrodes. *Analytica* **2023**, *4*, 513−526.
(44) Araújo, D. A.; Camargo, J. R.; Pradela-Filho, L. A.; Lima, A. P.; Munoz, R. A.; Takeuchi, R. M.; Janegitz, B. C.; Santos, A. L. A lab-made screen-printed electrode as a platform to study the effect of the size and functionalization of carbon nanotubes on the voltammetric determination of caffeic acid. *Microchem. J.* **2020**, *158*, No. 105297.
(45) Snari, R. M.; Alharbi, A.; Munshi, A. M.; Al-Ahmed, Z. A.; Aljuhani, E.; Alluhaybi, A. A.; Althagafi, I.; El-Metwaly, N. M. Zirconium Oxide Nanostructure Integrated Screen-Printed Mirabegron Voltammetric Sensors. *J. Electrochem. Soc.* **2023**, *170*, No. 113506.
(46) Abumelha, H. M.; Sayqal, A.; Snari, R. M.; Alkhamis, K. M.; Alharbi, A.; Al-Ahmed, Z. A.; El-Metwaly, N. M. Novel Deliberately Sensitive and Selective Tetrahydrozoline Voltammetric Sensors Integrated with a Copper Oxide Nanoparticle/Zeolite Platform. *ACS Omega* **2024**, *9*, 13458−13468.
(47) Compton, R. G.; Banks, C. E. *Understanding Voltammetry*; World Scientific, 2018.
(48) Bard, A. J.; Faulkner, L. R. *Electrochemical Methods Fundamentals and Applications*, 2nd ed.; Wiely: New York, 2000.
(49) Guideline, I. H. T. Stability Testing of New Drug Substances and Products. Q1A (R2), Current Step, 2003, 4.

https://doi.org/10.1021/acsomega.4c09110
ACS Omega 2025, 10, 2897−2907

(50) Omkar, S. D.; Komal, C.; Priti, M. J. Identification and structural characterization of major degradation products of tapentadol by using liquid chromatography−tandem mass spectrometry. *J. Liq. Chromatogr. Relat. Technol.* **2016**, *39*, 558−567.
(51) Guidance, F. D. A. *Guidance for Industry, Immediate Release Solid Oral Dosage Forms Scale-Up and Postapproval Changes: Chemistry, Manufacturing, and Controls. Vitro Dissolution Testing, and In Vivo Bioequivalence Documentation (SUPAC-IR)*; US Department of Health and Human Services, Food and Drug Administration, Center for Drug Evaluation and Research (CDER), 1995.
(52) Mazloum-Ardakani, M.; Manshadi, A. D.; Bagherzadeh, M.; Kargar, H. Impedimetric and potentiometric investigation of a sulfate anion-selective electrode: experiment and simulation. *Anal. Chem.* **2012**, *84*, 2614−2621.
(53) Norouzi, P.; Gupta, V. K.; Larijani, B.; Ganjali, M. R.; Faridbod, F. A new Methimazole sensor based on nanocomposite of CdS NPs−RGO/IL−carbon paste electrode using differential FFT continuous linear sweep voltammetry. *Talanta* **2014**, *127*, 94−99.
(54) Heli, H.; Zarghan, M.; Jabbari, A.; Parsaei, A.; Moosavi-Movahedi, A. A. Electrocatalytic oxidation of the antiviral drug acyclovir on a copper nanoparticles-modified carbon paste electrode. *J. Solid State Electrochem.* **2010**, *14*, 787−795.
(55) Zhang, Z.; Wang, E. *Electrochemical Principles and Methods*; Science Press: Beijing, 2000.
(56) Gosser, D. K. *Cyclic Voltammetry, Simulation and Analysis of Reaction Mechanisms*; Wiley VCH: New York, 1993.
(57) Elgrishi, N.; Rountree, K. J.; McCarthy, B. D.; Rountree, E. S.; Eisenhart, T. T.; Dempsey, J. L. A practical beginner's guide to cyclic voltammetry. *J. Chem. Educ.* **2018**, *95*, 197−206.
(58) Laviron, E. Theoretical study of a reversible reaction followed by a chemical reaction in thin layer linear potential sweep voltammetry. *J. Electroanal. Chem. Interfacial Electrochem.* **1972**, *39*, 1−23.
(59) Khadke, P.; Tichter, T.; Boettcher, T.; Muench, F.; Ensinger, W.; Roth, C. A simple and effective method for the accurate extraction of kinetic parameters using differential Tafel plots. *Sci. Rep.* **2021**, *11*, 8974.
(60) Jouikov, V.; Simonet, J. Electrochemical Reactions of Sulfur Organic Compounds. In *Encyclopedia of Electrochemistry: Online*, 2007.
(61) Guideline, I. H. T. Validation of Analytical Procedures: Text and Methodology. Q2 (R1), 2005, 1, 05.
(62) Görög, S. Critical review of reports on impurity and degradation product profiling in the last decade. *TrAC, Trends Anal. Chem.* **2018**, *101*, 2−16.
(63) Blessy, M. R. D. P.; Patel, R. D.; Prajapati, P. N.; Agrawal, Y. K. Development of forced degradation and stability indicating studies of drugs—A review. *J. Pharm. Anal.* **2014**, *4*, 159−165.
(64) Melveger, A. J.; Huynh-Ba, K. *Critical Regulatory Requirements for a Stability Program*; Springer, 2009; pp 9−19.
(65) Khan, H.; Ali, M.; Ahuja, A.; Ali, J. Stability testing of pharmaceutical products comparison of stability testing guidelines. *Curr. Pharm. Anal.* **2010**, *6*, 142−150.
(66) Baertschi, S. W.; Alsante, K. M.; Reed, R. A., Eds. *Pharmaceutical Stress Testing: Predicting Drug Degradation*; CRC Press, 2016.

https://doi.org/10.1021/acsomega.4c09110
ACS Omega 2025, 10, 2897−2907